Study on Magnetized RF Discharge with Very Small-Diameter*)

Toshiki NAKAGAWA, Yoshitake SATO, Eiko TANAKA, Hiraku IWAYA,
Daisuke KUWAHARA and Shunjiro SHINOHARA

Tokyo University of Agriculture and Technology, 2-24-16 Naka-Cho, Koganei, Tokyo 184-8588, Japan

(Received 1 December 2014 / Accepted 17 February 2015)

To investigate characteristics and estimate propulsion performance of a high-density radio frequency plasma with a very small diameter, we have developed the Small Helicon Device (SHD) and measured an electron density n_e, an ion velocity v_i and an emission intensity of Ar II under various conditions such as a discharge diameter (down to 3 mm), a mass flow rate and a gas species. Using quartz discharge tubes with inner diameter (i.d.) of 3, 10, 20 mm with an Ar gas, n_e of $(2.5 - 6) \times 10^{12}$ (estimated from optical measurement), $\sim 2.5 \times 10^{12}$ and $\sim 2.0 \times 10^{12}$ cm^{-3}, respectively, at -40 mm downstream from an excitation antenna was obtained. Using the 20 mm i.d. tube with a H_2 gas, $v_i \sim 40$ km/s was achieved in the presence of the magnetic field gradient.

Keywords: helicon plasma, small helicon device, electron density, emission intensity, ion velocity

DOI: 10.1585/pfr.10.3401037

1. Introduction

An electric propulsion system has a higher efficiency than a chemical one, and it suits for long term missions such as deep space explorations. However, a lifetime of the electric propulsion system, such as a Hall thruster, is limited by damage of electrodes contacting directly with a plasma. To solve this problem, we have proposed completely electrodeless helicon thruster using a high-density ($\sim 10^{13}$ cm^{-3}) helicon plasma [1–4]. In the case of producing the helicon plasma with a very small diameter, this source will contribute to the development of a lightweight and compact thruster such as an attitude control thruster, and that of a neutralizer. Here, simple thrusters can be seen in refs. [5–9]. The high-density, small plasma source may also have industrial applications, such as a coating of the inner wall of a thin tube.

In this paper, using the Small Helicon Device (SHD) [10, 11], we measured an electron density n_e and an ion velocity v_i using electrostatic probes to characterize small-diameter helicon plasmas. However, probes may disturb the plasma flow, therefore sometimes it is not suitable for measurements in very small diameter. Instead, optical measurements are useful. We measured an emission intensity of Ar II ($I_{\mathrm{Ar\,II}}$) with three small tubes, using a spectrometer to estimate n_e and compared this from a probe measurement. Here, if we can assume a Maxwellian electron energy distribution with a uniform electron temperature T_e, and the non-saturated phase of the ionizing plasma, which holds good in our experimental conditions, $I_{\mathrm{Ar\,II}}$ is proportional to n_e^2, and $\sqrt{I_{\mathrm{Ar\,II}}}/n_e$ should be constant [12].

Furthermore, to estimate propulsion performance of a small-diameter plasma, we measured n_e and ion velocity v_i (relating to a thrust and a specific impulse) using a 20 mm diameter tube with different gas species of He and H_2 in addition to Ar. Here, we can expect higher ion velocity with the lighter ions if the axial potential drop is the same.

2. Experimental Setup

Figure 1 shows a photograph and a schematic drawing of SHD. A small-diameter, quartz discharge tube was connected to a vacuum chamber (SUS316) in inner diameter of 165 mm and an axial length of 865 mm, pumped by a rotary pump (CVD-050A, ULVAC) through a turbo-molecular pump (TG200, Osaka Vacuum). Here, various diameter discharge tubes can be connected to the vacuum gauge port adapters [left sides of Figs. 1 (a) and (b)]. Pirani gauge and ion one were installed at the head of the discharge tube and also at the end of the chamber. The base pressure in the vacuum chamber was $\sim 7 \times 10^{-5}$ Pa. Quartz

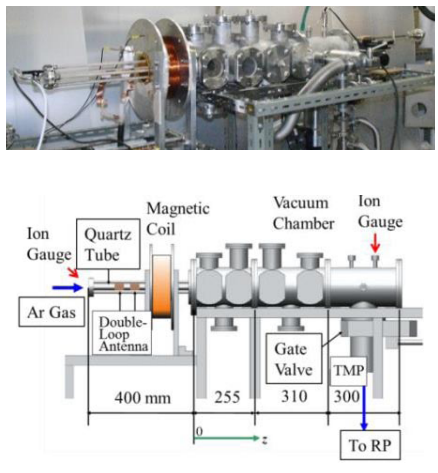

Fig. 1 (a) Photograph and (b) schematic drawing of SHD.

author's e-mail: yukasenzai@gmail.com

*) This article is based on the presentation at the 24th International Toki Conference (ITC24).

tubes have inner diameters (i.d.s) of 3, 10 and 20 mm with axial lengths of 453 mm. The radio frequency (rf) antenna was a double-loop type at $z = -170 \sim -230$ mm, where $z = 0$ is defined in Fig. 1 (b), made of copper plates with a thickness of 0.2 mm and a width of 40 mm.

An rf power supply (T145-6326CK, THAMWAY) can deliver rf power up to 2 kW with an rf frequency of 0.3 - 13.56 MHz, through a matching box (T020-6326AK, THAMWAY). A directional coupler in the matching box was connected to an oscilloscope (TDS2024B, Tektronix) to measure rf power P_{rf} (subtracting the reflecting power from the incident one). Gases can be fed by two mass flow controllers (SEC-400MK3, HORIBASTEC: 0 - 30 sccm, 0.1 sccm step, and SEC-Z512KX, HORIBASTEC: 0 - 1 sccm, 0.01 sccm). To accelerate plasmas with the magnetic field gradient and stabilize them with a better confinement, a handmade solenoid coil (90 mm i.d., 360 mm outer diameter and 120 mm axial length with 400 turns of winding coils) was used; the coil can produce the axial magnetic field of 28 G/A in the coil region and the typical operating coil current I is 20 A. To have reproducible discharges in the case of i.d. of 3 mm tube, a hot filament was installed in the vacuum chamber.

For the measurement of n_e, T_e and v_i, a single probe, a double probe and a Mach probe with a data logger (MEMORY HiCORDER 8855, 20 MS/s, HIOKI) were used. Plasma emission intensities were measured by a CCD spectrometer (HR2000+, Ocean Optics, wavelength range: 360 - 792 nm, resolution: 0.45 nm). We chose 434.94 nm of the wavelength of Ar II. As was mentioned, n_e can be estimated, since it is proportional to $\sqrt{I_{Ar\,II}}$. The electron temperature, which is also needed to estimate n_e and v_i, was assumed to be 5 eV (typical value) in those measurements.

3. Experimental Results

Figures 2 and 3 show n_e and $I_{Ar\,II}$ at $z = -60$ mm (in the quartz tube and downstream of the rf antenna), respectively, as a function of P_{rf} with an i.d. of 20 mm tube with the Ar gas (the product of the effective solid angle and path length is $L = 0.959$ str.mm). A solenoid coil was placed at $z = -155$ mm, to produce the magnetic field. Although n_e did not reach 10^{13} cm^{-3}, n_e and $I_{Ar\,II}$ increased with P_{rf} under all Flow Rate FR and magnetic coil current I. In the case of FR of 20 sccm without the magnetic field, n_e jump by a factor of ~ 20 was observed at $P_{rf} \sim 200$ W, and $I_{Ar\,II}$ was too weak to be observed before the density jump. The jump is considered to be a mode transition from a Capacitively Coupled Plasma (CCP) to an Inductively Coupled Plasma (ICP). $I_{Ar\,II}$ showed the opposite dependence on the magnetic field.

Figures 4 and 5 show T_e by a double probe and the ratio of the square root of $I_{Ar\,II}$ to n_e as a function of P_{rf} respectively. T_e decreased slightly with P_{rf} especially without the magnetic field. Since $I_{Ar\,II}$ is proportional to n_e^2,

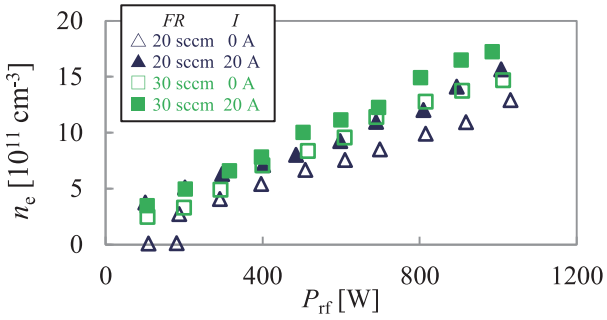

Fig. 2 n_e vs. P_{rf} with a 20 mm i.d. tube, changing FR and I ($z = -60$ mm).

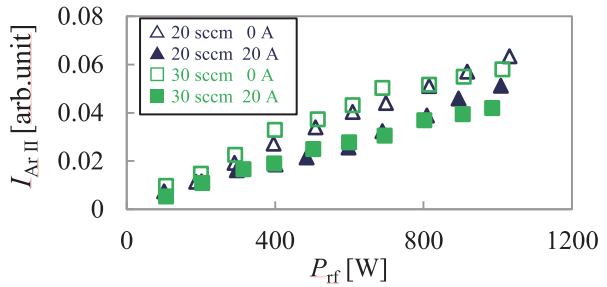

Fig. 3 $I_{Ar\,II}$ vs. P_{rf} with a 20 mm i.d. tube, changing FR and I ($z = -60$ mm).

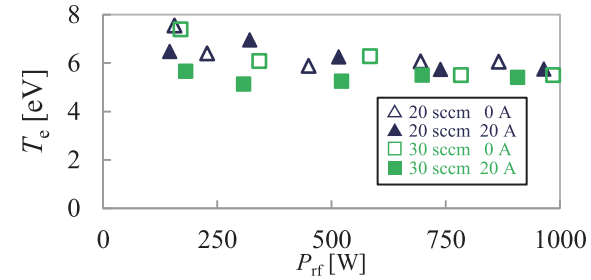

Fig. 4 T_e vs. P_{rf} with a 20 mm i.d. tube, changing FR and I ($z = -60$ mm).

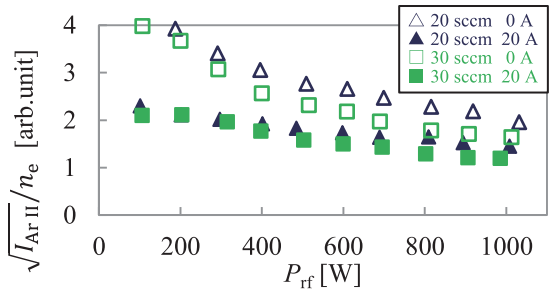

Fig. 5 $\sqrt{I_{Ar\,II}}/n_e$ vs. P_{rf} with a 20 mm i.d. tube, changing FR and I ($z = -60$ mm).

$\sqrt{I_{Ar\,II}}/n_e$ should be constant if uniform T_e is assumed, as was mentioned. However, $\sqrt{I_{Ar\,II}}/n_e$ decreased with P_{rf} and larger in cases of without the magnetic field under low rf powers. This may be due to the fact that $I_{Ar\,II}$ is proportional to the cross section, which increases strongly with T_e [13].

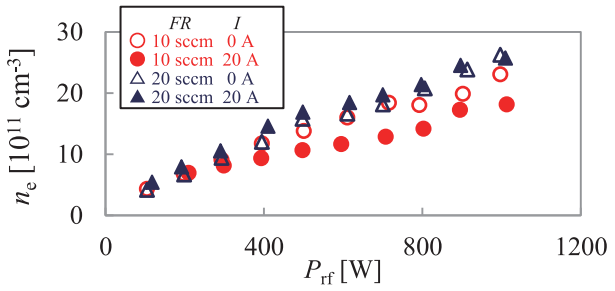

Fig. 6 n_e vs. P_{rf} with a 10 mm i.d. tube, changing FR and I (z = − 60 mm).

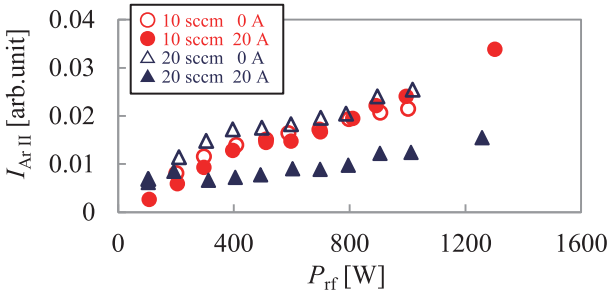

Fig. 7 $I_{Ar\ II}$ vs. P_{rf} with a 10 mm i.d. tube, changing FR and I (z = − 60 mm).

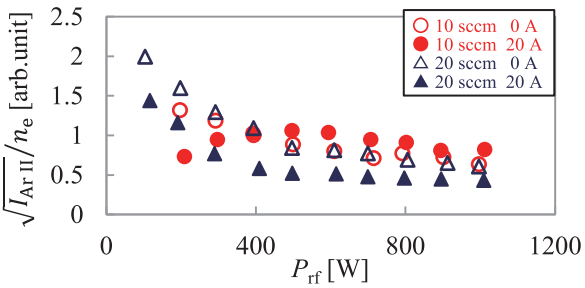

Fig. 8 $\sqrt{I_{Ar\ II}}/n_e$ vs. P_{rf} with a 10 mm i.d. tube, changing FR and I (z = −60 mm).

Figures 6 and 7 show n_e and $I_{Ar\ II}$ at z = −60 mm as a function of P_{rf} with i.d. of 10 mm tube using an Ar gas, respectively (L: 0.452 str.mm). A solenoid coil was placed at z = −155 mm. Although this shows larger n_e with 10 mm i.d. than that of 20 mm i.d. case, this density range can be expected from a plasma production efficiency [14]. $I_{Ar\ II}$ is lower due to a lower receiving volume, and the density jump was not observed. In the case of FR of 10 sccm and I = 20 A, n_e was the lowest and $\sqrt{I_{Ar\ II}}/n_e$ (shown in Figure 8) also decreased with P_{rf}. This value of $\sqrt{I_{Ar\ II}}/n_e$ is consistent with that in the case of 20 mm i.d., considering also L using a fiberscope of the monochromator.

Figure 9 shows $I_{Ar\ II}$ at z = −60 mm as a function of P_{rf} with i.d. of 3 mm using with an Ar gas (L: 0.072 str.mm). A solenoid coil was placed at z = −155 mm. Although we have succeeded in rf plasma discharges, n_e could not be measured due to the comparable size of the probe to the quartz tube. The discharge was unstable and plasmas could not be produced at P_{rf} < 700 W. The plasma

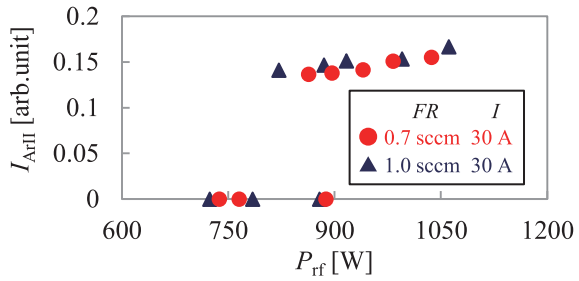

Fig. 9 $I_{Ar\ II}$ (z = −60 mm) vs. P_{rf} for 3 mm i.d. tube changing FR.

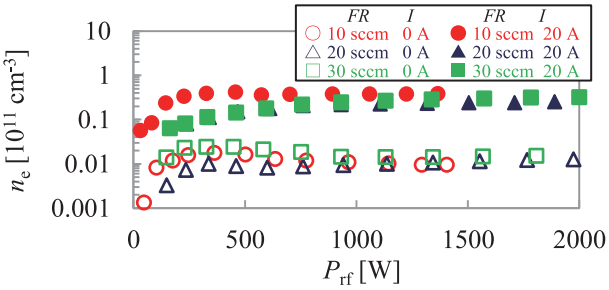

Fig. 10 n_e vs. P_{rf} with a He gas, changing FR and I (z = −40 mm).

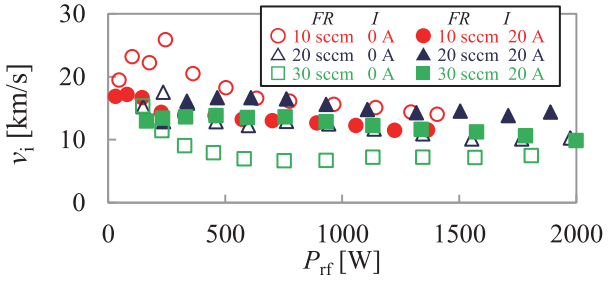

Fig. 11 v_i vs. P_{rf} with He gas, changing FR and I (z = −40 mm).

plume was localized and did not reach the optical measurement point of z = −60 mm in the lower P_{rf} region. Here, $I_{Ar\ II}$ ~ 0.15 for P_{rf} ~ 1,000 W was obtained at 0.7 and 1.0 sccm. From the results with 10 and 20 mm i.d., considering L, we can estimate that n_e for i.d. of 3 mm was (2.5 - 6) × 10^{12} cm^{-3}.

Next, we will show the plasma performance including the ion velocity, changing gas species. A solenoid coil was placed at z = −90 mm. Figures 10 and 11 show n_e and v_i at z = −40 mm (in the quartz tube region and away from the antenna region, having the large magnetic field gradient) as a function of P_{rf} with i.d. of 20 mm tube using a He gas, respectively. Here, for a Mach probe measurement, an unmagnetized model was used (model constant κ = 1.26) [15, 16]. In the experiment using the Ar gas, n_e of ~ 3 × 10^{12} cm^{-3} and v_i of ~ 1.5 km/s was obtained for P_{rf} ~ 1,500 W with and without magnetic fields, respectively. In He discharges, n_e ~ 3 × 10^{10} and 10^9 cm^{-3} was obtained for P_{rf} ~ 1,500 W with and without the magnetic fields, respectively. Here, n_e was lower than the case of Ar, and plasma emission intensities were weaker, because the

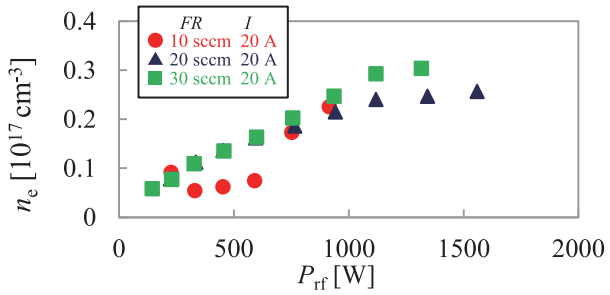

Fig. 12 n_e vs. P_{rf} with a H_2 gas, changing FR and $I(z = -40\,\text{mm})$.

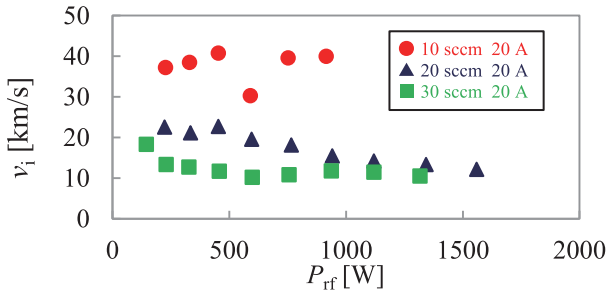

Fig. 13 v_i vs. P_{rf} with a H_2 gas, changing FR and $I(z = -40\,\text{mm})$.

first ionization energy of He is higher than Ar. Since the molecular weight of He is about one tenth of that of Ar, v_i of He is much higher than Ar; with $P_{rf} \sim 1{,}500$ W, $v_i \sim 15$ km/s was obtained (typical ion Mach number $M_i \sim 1.5$) and saturated at $P_{rf} > 200$ W under all conditions.

Figures 12 and 13 show n_e and v_i at $z = -40$ mm as a function of P_{rf} with i.d. of 20 mm with a H_2 gas, respectively. Without the magnetic field ($I = 0$), n_e was low and discharge was unstable, therefore we could not measure plasma parameters in the quartz tube region. Although the first ionization energy of H_2 is lower than that of Ar, n_e of H_2 was lower than that of Ar because H_2 is a diatomic molecule [17]. With FR of 20 sccm and I of 20 A, $v_i \sim 40$ km/s ($M_i \sim 1.8$) was obtained, and it is the highest velocity, leading to the specific impulse of $\sim 4{,}000$ s for protons. In the cases of Ar and He, v_i did not change so much for all the conditions (~ 1.5 km/s with an Ar ion and ~ 12 km/s with a He ion). However, in the case of H_2, v_i increased at lower FR, which is considered as a reduction of collision frequency due to a low pressure.

4. Concluding Remarks

We have obtained the following results with very small diameters in magnetized rf discharges.

1. High-density plasmas were produced with small diameter discharge tubes; i.d. of 3, 10 and 20 mm with an Ar gas. By the Langmuir probe and the spectrometer, n_e and $I_{Ar\,II}$ were measured. Here, T_e was also measured and showed a slight decrease with P_{rf}.
2. High-density plasmas with high flow velocities were measured by a Mach probe in the case of i.d. of 20 mm using He and H_2 gases in addition to Ar one. Here, n_e of $\sim 3 \times 10^{10}$ cm^{-3} and v_i of ~ 40 km/s was obtained using a H_2 gas at $FR = 10$ sccm, $I = 20$ A and $P_{rf} \sim 1{,}000$ W.
3. In the cases of i.d.s of 10 and 20 mm, $\sqrt{I_{Ar\,II}}/n_e$ was not constant and decreased with an increase of P_{rf}, which can be considered that T_e was lower in the higher P_{rf} region than the lower one, ascertained by a probe measurement. In the case of i.d. 3 mm, where a probe measurement is impossible, n_e was estimated to be $(2.5\text{-}6) \times 10^{12}$ cm^{-3} from an optical measurement.

As for a thrust performance, a rough estimate shows that the total thrusts F_{total} (= ion thrust F_i + neutral thrust F_0) are on the order of ~100, 10 and 10 μN for Ar, He and H_2 gases, respectively. Although ion velocity is high, effective specific impulse I_{sp} ($=F_{total}/\dot{m}_0 g$, where $\dot{m}_0$: neutral mass flow rate, g: acceleration of gravity) is low (< 100 s) due to a high neutral density (low ionization degree).

In this experiment, we have measured n_e and v_i with small diameters. To measure them with no perturbation to very small diameter plasmas, we are planning to use a fine resolution spectrometer (focal length 1.5 m, minimum resolution ~ 0.005 nm). In addition, to measure n_e and T_e, we are developing a code based on Collisional Radiative (CR) model, calculating line intensity ratios using Ar I lines, and estimate n_e and T_e [12, 18].

[1] R.W. Boswell, Phys. Lett. **33A**, 457 (1970).
[2] S. Shinohara, Jpn. J. Appl. Phys. **36**, 4695 (1997).
[3] R.W. Boswell and F.F. Chen, IEEE Trans. Plasma Sci. **25**, 1229 (1997).
[4] F.F. Chen and R.W. Boswell, IEEE Trans. Plasma Sci. **25**, 1245 (1997).
[5] C. Charles, J. Phys. D, Appl. Phys. **42**, 18 (2009).
[6] E. Ahedo and M. Merino, Phys. Plasmas **17**, 073501 (2010).
[7] K. Takahashi, C. Charles, R.W. Boswell and T. Fujiwara, Phys. Rev. Lett. **107**, 35002 (2011).
[8] S. Shinohara *et al.*, IEEE Trans. Plasma Sci. **42**, 1245 (2014).
[9] A. Fruchtman, Phys. Rev. Lett. **96**, 065002 (2006).
[10] D. Kuwahara, A. Mishio, T. Nakagawa and S. Shinohara, Rev. Sci. Instrum. **84**, 103502 (2013).
[11] T. Nakagawa, S. Shinohara, D. Kuwahara, A. Mishio and H. Fujitsuka, JPS Conf. Ser. **1**, 1245 (2014).
[12] S. Waseda, H. Fujitsuka, S. Shinohara, D. Kuwahara, M. Sakata and H. Akatsuka, Plasma Fusion Res. **9**, 3406125 (2014).
[13] T. Shoji, Private communication.
[14] S. Shinohara *et al.*, Phys. Plasmas **16**, 057104 (2009).
[15] M. Hudis and L.M. Lidsky, J. Appl. Phys. **41**, 5011 (1970).
[16] K.S. Chung, I.H. Hutchinson, B. Labombard and R.W. Boswell, Phys. Fluids **B1**, 2229 (1989).
[17] H. Kikuchi, Y. Hukui, Y. Sakawa and T. Shoji, Phys. Plasmas **10**, 521 (2003).
[18] J. Vlček, J. Phys. D, Appl. Phys. **22**, 623 (1989).